

Experimental Demonstration of a High-Resolution Ultra-Wide-Swath Imaging Mode for Ship Monitoring Based on Continuous PRF Variation and Alternated Up- and Down-Chirp Waveforms

Nertjana Ustalli, Maxwell Nogueira Peixoto, Thomas Kraus, Ulrich Steinbrecher, Gerhard Krieger, and Michelangelo Villano

German Aerospace Center (DLR), Microwaves and Radar Institute, Germany

Abstract

Maritime surveillance using synthetic aperture radar (SAR) calls for both a wide swath and high resolution. This allows for the monitoring of wide areas with high detection probabilities and low false alarm rates at short time intervals. Ambiguous SAR modes, such as the staggered ambiguous mode utilizing continuous variation of short pulse repetition intervals and the low pulse repetition frequency mode, have proven effective for ship monitoring. This is especially true in remote offshore regions. Both modes, can image a wide swath with high azimuth resolution without the need of digital beamforming or multiple apertures, as ambiguities of the ships can be tolerated. Building upon the successful demonstration of the staggered ambiguous mode using experimental data acquired by the TerraSAR-X satellite, this paper presents a further demonstration. We achieve ultra-wide swath imaging, extending the ground swath width from 110 to 160 km, while maintaining the same high azimuth resolution of 2.2 m. Furthermore, we extend the application of the ambiguous mode to coastal areas. This achievement is accomplished by introducing in the staggered ambiguous mode an alternation of up- and down-chirp waveforms. An experimental acquisition was carried out over a scene located in the North Sea and including part of the Dutch coast. Compared to the TerraSAR-X ScanSAR mode, a swath width larger by 50% and an azimuth resolution eight times better are achieved. Despite the presence of first-order range ambiguities caused by land scatterers, the detection of small ships remains feasible, as these ambiguities are very blurred and manifest as noise-like disturbances. These results are of fundamental importance for incorporating the ambiguous modes into existing and future SAR systems as an efficient additional mode for ship monitoring, suitable for both open sea and coastal surveillance.

1 Introduction

Synthetic aperture radar (SAR) images have great potential for observing and monitoring the maritime environment, benefiting applications like maritime traffic control, pollution monitoring, fisheries, smuggling prevention, and defence purposes [1]. User requirements include persistence, high detection performance, and responsiveness. Mapping wider swaths improves observation frequency, while higher resolution SAR images enhance detection performance by providing more favourable statistics. On-board processing reduces latency for improved responsiveness. However, wide-swath coverage and high-resolution imaging pose contradicting requirements on the pulse repetition frequency (PRF). Controlling range ambiguities requires a pulse repetition interval (PRI) greater than the time needed to collect returns from the entire illuminated swath. A large PRI (low PRF) limits the unambiguous Doppler bandwidth and therefore the achievable azimuth resolution if azimuth ambiguities have to be controlled [2]. A wide swath can also be mapped with ScanSAR or Terrain Observation by Progressive Scans (TOPS), but the azimuth resolution is still impaired. Digital beamforming (DBF) and multiple aperture recording are promising techniques that overcome these limitations and achieve high-resolution wide-swath images. However, they also involve higher system complexity and costs. In [3], we have proposed two high-resolution wide-swath ship monitoring modes that “tolerate” ambiguities and are suitable for offshore region surveillance: the low PRF mode, which “tolerates” azimuth ambiguities of the ships, and staggered (high PRF) ambiguous

mode, which “tolerates” range ambiguities of the ships. Both modes map wide swaths by using a wide elevation beam on both transmit and receive obtained through tapering [4]. The low PRF mode collects echoes from a wide swath with a PRF smaller than the nominal Doppler bandwidth, achieving high azimuth resolution by processing the full Doppler bandwidth. The staggered (high PRF) ambiguous mode uses a sequence of distinct PRIs with a mean PRF greater than the Doppler bandwidth. A larger swath, but a coarser azimuth resolution, can be obtained with a ScanSAR mode with six sub-swaths that tolerates azimuth ambiguities, as proposed by NovaSAR [5]. This, however, leads to the detection of only medium to large ships with a false alarm rate of 10^{-7} .

In our previous work [3], we demonstrated that the ambiguous SAR modes enable the detection of small ships, i.e., of $21 \text{ m} \times 6 \text{ m}$ size, by imaging a wide swath of up to 240 km with a probability of detection of at least 0.85, while also keeping the same false alarm rate as NovaSAR, corresponding to one false alarm over a 1000 km^2 area. The ambiguous modes therefore achieve a swath similar to that of a ScanSAR mode and a resolution cell of 2 m^2 , similar to that of a spotlight mode. For a ScanSAR mode that images the same swath (100 km ground swath as in TerraSAR-X) with a coarser resolution, ($18.5 \text{ m} \times 5 \text{ m}$ as in TerraSAR-X), the probability of detection, assuming the same ship size and false alarm rate as in the ambiguous modes would be less than 0.3 [3].

In [6] an experimental TerraSAR-X acquisition in staggered (high PRF) ambiguous mode imaging a ground

swath of 110 km far from the coast with 2.2 m azimuth resolution has been performed over the North Sea. Data have been processed and the detection results have been successfully validated using automatic identification system data. The impact of the TerraSAR-X technical limitations on the selection of non-optimal system parameters for ship detection application, such as the PRI sequence, pulse length, and the chirp bandwidth has been thoroughly discussed in [6]. The use of a non-optimal PRI sequence has resulted in range ambiguities from ships still being above the detection threshold and their specific signature due to the PRI variation has still allowed for a discrimination between the ships and their ambiguities.

Building upon the findings presented in [6], this paper reports the results of a further experimental TerraSAR-X acquisition conducted in the North Sea along the Dutch coast. The acquisition features the staggered ambiguous mode jointly with alternating up- and down-chirps. The paper addresses the rationale behind the proposed mode, the design of the TerraSAR-X experiment, data processing, ship detection, and discusses the impact of both first-order and second-order range ambiguities associated with land scatterers.

2 Staggered ambiguous mode with alternating up- and down-chirps concept

The staggered (high PRF) ambiguous mode in [3] and the staggered SAR system employing DBF [7] exhibit notable differences, which are discussed in [6]. Here, the rationale behind the staggered ambiguous mode with alternating up- and down-chirps will be shortly recalled. The upper panel of **Figure 1** shows the simplified acquisition geometry. A wide elevation transmit beam illuminates a wide swath and in receive the echoes are collected with the same wide beam used in transmit. The middle part of **Figure 1** depicts the transmission and reception of radar echoes for the simplified case of a sequence of $M = 5$ PRIs with a linear decreasing trend. On the upper part of the middle panel, the transmitted alternating up- and down-chirp pulses, separated by the varying PRIs, are displayed on a time axis. Ten pulses are transmitted, i.e., the PRI sequence is repeated twice. Each transmitted pulse is represented by different colours with the circled number indicating the pulse index; the up-chirp pulses are denoted with the symbol U and the down-chirp pulses are denoted with the symbol D . Immediately below, the received echoes corresponding to the first two transmitted pulses, i.e., pulse indices 0 (representing an up-chirp) and 1 (representing a down-chirp), are shown on the same time axis. The radar echoes from the sea clutter are displayed with the same colours as the corresponding transmitted pulses. The radar echo return from a ship at a slant range R_0 (for simplicity, we assume the ship is not moving) overlaps to the echo return from the sea clutter. It is marked in red, with the upper circled number followed by the symbol U or D indicating the corresponding transmitted pulse. It is important to note that while we receive the desired radar echo of the ship at slant range R_0 from pulse number 0, marked in red, we will also receive

an ambiguous return from pulse number 1, shown in white with upper circled number 1 and symbol D . This is because the receive echo window, the time interval during which the receiver is turned on and can receive radar echoes, is typically much shorter than the duration of the radar echo from the illuminated swath. This is also true for the sea clutter returns, which will overlap, as shown in the middle panel of **Figure 1**.

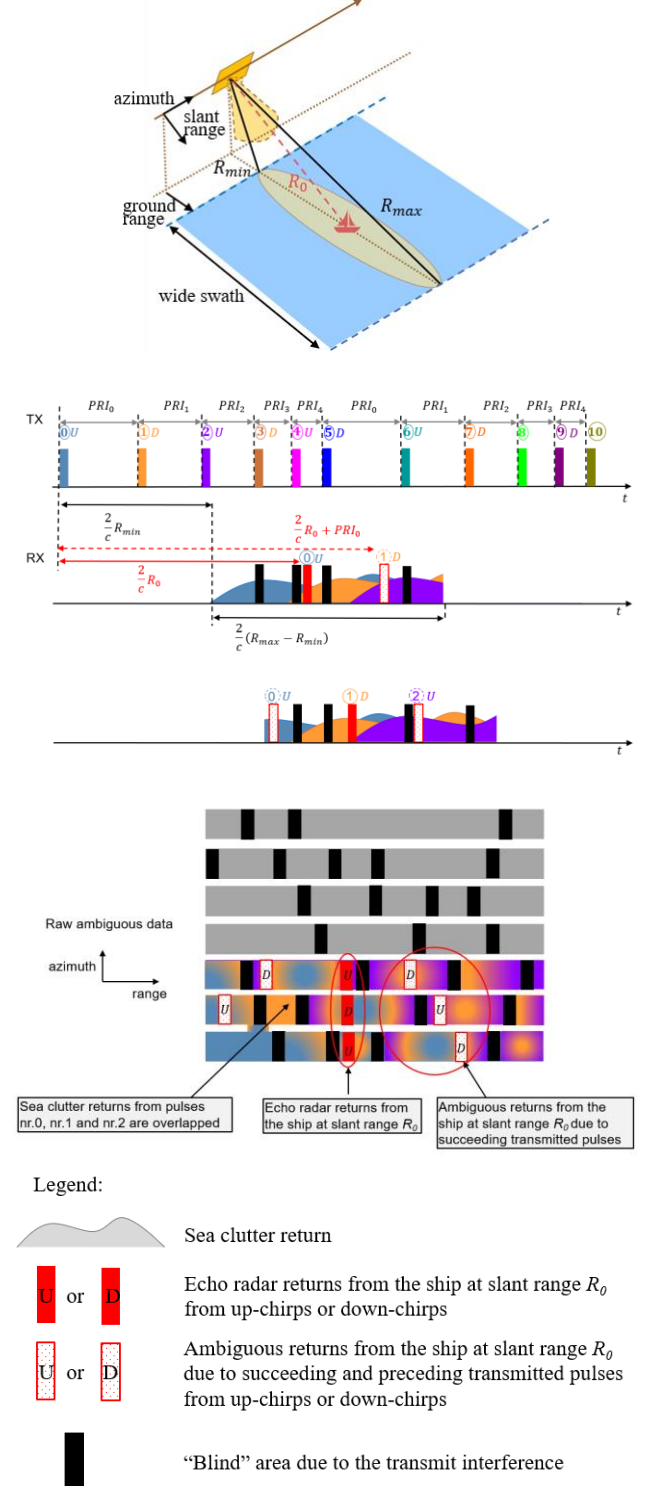


Figure 1 Top: Simplified acquisition geometry. Middle: Transmitted pulses and corresponding received echoes. Bottom: Raw data obtained by rearranging side by side the received echoes.

The received echoes are then rearranged, i.e., shifted at the same reception time (see bottom panel of **Figure 1**). As a result, the received radar echoes from the ship are at the same slant range R_0 for all range lines, while its ambiguous returns are located at different ranges for different range lines, as the time difference between the transmit pulses continuously varies. Following the range compression of the rearranged data, achieved by alternating up- and down-chirps in **Figure 1**, the ship at the slant range R_0 will be focused in range. In contrast its first-order range ambiguity (along with all the odd-order range ambiguities) will be smeared in range during the range compression operation. This smearing occurs because of the mismatch between the ambiguous returns, alternating between down- and up-chirps, and the reference signal, alternating between up- and down-chirps in the example shown in **Figure 1**. The smearing factor of the odd ambiguities in range is proportional to the compression ratio of the transmitted chirp [8]. Furthermore, after azimuth compression, the ambiguous energy of both even and odd-order ambiguities, due to PRI variation, is incoherently integrated and will spread almost uniformly across the whole Doppler spectrum [8]. The same applies to sea clutter echoes or land scatterers. This results in an increase in the disturbance level in the region affected by the ambiguities, which must be considered when selecting the threshold to detect the ships.

Due to the radar's inability to receive while transmitting, some "blind areas" will be present on the received data with width equal to the pulse length plus the additional guard times that are necessary in the radar hardware to separate the pulse transmission from the receiving window. These "blind areas" are marked in black in the middle and last panel of **Figure 1**. As the PRI is continuously varied, the locations of the blind areas will be different for each range line, as they are related to the time distances between the transmitted pulses.

3 TerraSAR-X experiment

TerraSAR-X is a conventional phased-array SAR that can be operated in staggered SAR mode, because it has 512 different PRIs and can be commanded to transmit pulses based on a sequence of M distinct PRIs that then repeats periodically, as demonstrated in [7].

As test site for the demonstration, an area in the North Sea along the Dutch coast was selected. The chosen elevation beam illuminates a 160 km ground swath with minimum and maximum look angles of 53.74° and 56.67° , respectively. The 160 km ground swath is not defined by the 3 dB antenna beamwidth, but by a larger beamwidth, as TerraSAR-X still provides adequate noise equivalent sigma zero (NESZ), ensuring a sufficient signal-to-noise ratio for effective ship detection across the wide swath. **Figure 2** shows the test site, with the red rectangle representing the 66 km ground swath defined by the 3 dB antenna beamwidth. The green rectangle outlines the 160 km ground swath area of the acquired SAR image, which includes a portion of the Dutch coast.

Once the beam has been selected, other system parameters such as the PRI sequence, the pulse length τ , and the chirp

bandwidth B_r , has to be chosen to ensure the best ship detection performance while respecting the TerraSAR-X technological constraints. The three main constraints of TerraSAR-X include the maximum echo window length, the maximum allowed duty cycle, and the limited number of selectable PRIs. For a pulse length of 45 μ s, a chirp bandwidth of 100 MHz is it possible to design a sequence of $M = 43$ PRIs that satisfies all the constraints, as for the experiment in [6], with a mean PRF of the sequence of 3525 Hz greater than the 3 dB Doppler bandwidth (2807 Hz) and mean duty cycle of 16.1%. A ground range resolution of 1.75 m at near range and an azimuth resolution of 2.2 m are achieved if no weighting windows are used during processing.

The location of the missing samples, i.e., blind areas, in the raw data for one cycle of the selected PRI sequence is depicted in **Figure 3**, i.e., areas in black, using the blockage diagram approach as in [9]. This will be exploited in the next section to rearrange the raw data.

The detection performance depends on the ship size and the statistics of the background disturbance. In the case of the staggered (high PRF) ambiguous mode, this disturbance includes not only thermal noise and sea clutter returns but also requires a careful consideration of the effects of range ambiguities caused by land scatterers and large ships. The NESZ is evaluated for the selected antenna beam and shown as a function of ground range in **Figure 4**; it ranges from -14 dB at the swath center to about 10 dB at near and far range and is much worse than for typical TerraSAR-X stripmap (or ScanSAR) acquisitions.

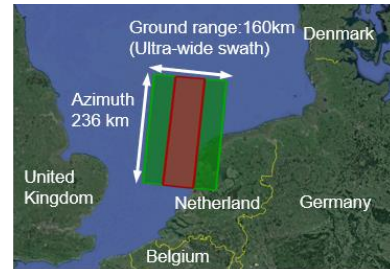


Figure 2 North Sea test site selected for the experimental acquisition. The green rectangle delimits the 160 km ground swath area of the acquired SAR image, while the red rectangle delimits the area within the 66 km ground swath from the 3 dB antenna beamwidth.

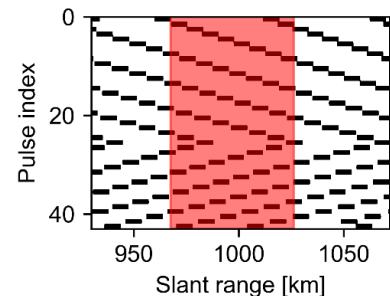


Figure 3 Location of the missing samples in the raw data for the imaged 150 km swath in slant range (160 km ground range swath) and 43 transmitted pulses (one cycle of PRI variation). The red rectangle highlights the 58 km swath in slant (66 km ground swath) within the 3 dB antenna beamwidth.

If thermal noise were the dominant disturbance component, the probability of detecting a medium-sized ship measuring $40 \text{ m} \times 8 \text{ m}$ within the 160 km ground swath would be greater than 0.5, given a false alarm rate of 1.26×10^{-9} , corresponding to one false alarm over a $100\,000 \text{ km}^2$ area, as shown in **Figure 5**. For small ships measuring $21 \text{ m} \times 6 \text{ m}$, the probability of detection exceeds 0.5 within a 120 km ground swath for the same false alarm rate. This approximation holds true for NESZ values greater than 0 dB, as discussed in [10], and in areas where range ambiguities from land scatterers are absent.

While the results in **Figure 5** refer to the case of only thermal noise, it is important to discuss some aspects related to the range ambiguities that will impact performance. The two-dimensional (2-D) impulse response function (IRF) of the first-order range ambiguity for a point scatterer, for the selected PRI sequence with alternating up- and down-chirps is shown in **Figure 6** (a). We note that the ambiguity is smeared both in range and azimuth appearing as noise like disturbance. This is unlike the scenario where no alternation between up- and down-chirps is employed, as illustrated in **Figure 6** (b). Moreover, upon comparing the range and azimuth cuts depicted in **Figure 6** (c), we observe a decrease in the intensity level of the first-order range ambiguity when the alternation between up- and down-chirps is employed, approximately 13 dB lower than when it is not employed. Conversely, the second-order range ambiguity for the selected PRI sequence, combined with the alternation of up- and down-chirps, will exhibit the same signature as in **Figure 6** (b). In this case, they appear as a set of lines parallel to the azimuth direction but with lower intensity values.

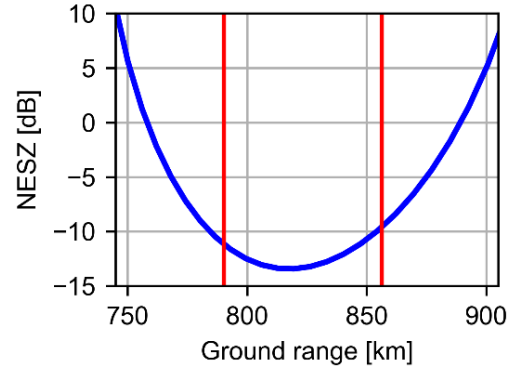


Figure 4 NESZ as a function of the ground range for the selected antenna beam. The red vertical lines delimit the 66 km ground swath defined by the 3 dB antenna beam-width.

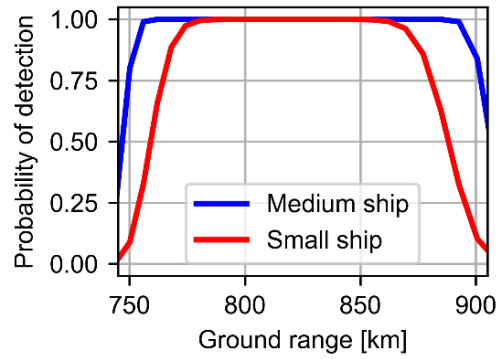


Figure 5 Probability of detection of a medium ship of $40 \text{ m} \times 8 \text{ m}$ size and small ship of $21 \text{ m} \times 6 \text{ m}$ size as function of the ground range for a probability of false alarm of 1.26×10^{-9} .

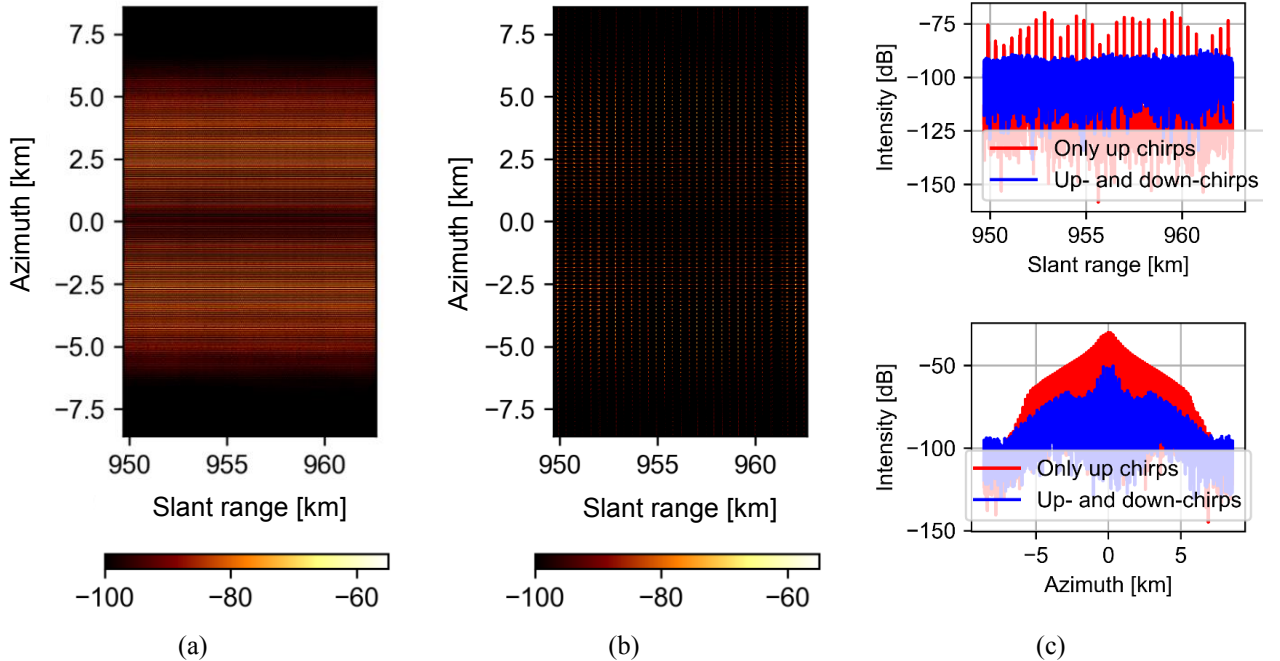


Figure 6 (a) 2-D IRF of the first-order range ambiguous point scatterer obtained by 2-D simulation when alternating up- and down-chirps are transmitted. Peak value is -43 dB . (b) 2-D IRF of the first-order range ambiguous point scatterer obtained by 2-D simulation when only up chirps are transmitted as in [6]. Peak value is -30 dB . (c) Comparison of a cut along azimuth and range between the first-range ambiguity with and without alternating up-and down-chirps.

4 Data processing and results

The TerraSAR-X experimental acquisition in staggered ambiguous mode with additional up- and down-chirp alternation has been performed on July 31, 2023 over the North Sea. The sequence of 43 PRIs is repeated 2800 times. The echoes, received by the radar between consecutive transmitted pulses, have different duration, as different PRIs are employed. Unlike in a SAR with constant PRI, the first samples of the received echoes correspond in a staggered SAR system to different slant ranges. Those echoes have therefore to be rearranged in a two-dimensional matrix with coordinates slant range and azimuth. This rearrangement associated each sample of radar echo with its corresponding range, utilizing the missing sample diagram shown in **Figure 3**. Please note that each received echo contains not only the desired return, but also the returns of preceding and succeeding pulses as they arrive back at the radar at the same time.

After rearrangement, range compression is performed using alternating up- and down-chirps. Subsequently, the data are resampled on a uniform grid, following the procedures outlined in [11]. It is important to note that in this scenario, due to the alternation of up- and down-chirps between the transmitted pulses, resampling of the rearranged raw data is not possible, despite resulting in a lower side lobe ratio. Range cell migration correction and azimuth compression are then performed. **Figure 7** shows the intensity of the focused data for the entire scene, covering over 37 760 km², where the strong returns from ships along with the coastline and the first- and second-order range ambiguities from the coast are visible. The red and green rectangles highlight the areas affected by the first-order and second-order range ambiguities from land scatterers. The smearing of the first-order range ambiguities and its appearance as noise-like disturbance are visible. On the other hand, the second-order range ambiguities from the land scatterers appears as a set of lines parallel to the azimuth and have a signature similar to the 2-D IRF shown in **Figure 6** (b). **Figure 8** provides a closer look of three medium and small ships within the scene. In **Figure 8** (b) is shown a small ship overlapped to the first-order range ambiguities from the land scatterers inside the red rectangle shown in **Figure 7**. Furthermore, refocusing of the range ambiguities of the large ships and their removal following the same approach proposed in [12] could be useful and investigated in the future.

5 Conclusions

An experimental TerraSAR-X acquisition in staggered ambiguous mode with alternating up- and down-chirps imaging a ground swath of 160 km with 2.2 m azimuth resolution has been performed over the North Sea along the Dutch coast. Data have been processed and it is shown that the proposed mode is effective for both open sea and coastal surveillance. The exploitation of ambiguous modes can go beyond the monitoring of ships and be extended to other applications, such as deformation monitoring using permanent scatterers interferometry, currently under investigation.

6 Literature

- [1] J. Krecke, M. Villano, N. Ustalli, A. C. M. Austin, J. E. Cater, and G. Krieger, "Detecting ships in the New Zealand exclusive economic zone: Requirements for a dedicated smallsat SAR mission," *IEEE J. Sel. Topics Appl. Earth Observ. Remote Sens.*, vol. 14, pp. 3162–3169, 2021.
- [2] C. Curlander and R. N. McDonough, *Synthetic Aperture Radar Systems and Signal Processing* (Wiley Series in Remote Sensing), Boulder, Colorado: Pocket Ventures LLC, 1991.
- [3] N. Ustalli, M. Villano, "High-Resolution Wide-Swath Ambiguous Synthetic Aperture Radar Modes for Ship Monitoring," *Remote Sensing*, vol. 14, no. 13, p. 3102, Jun. 2022, doi: 10.3390/rs14133102.
- [4] M. Villano, G. Krieger and A. Moreira, "Advanced spaceborne SAR systems with planar antenna," *2017 IEEE Radar Conference (RadarConf)*, Seattle, WA, USA, 2017, pp. 0152–0156.
- [5] M. Cohen, A. Larkins, P. L. Semedo and G. Burbidge, "NovaSAR-S low cost spaceborne SAR payload design, development and deployment of a new benchmark in spaceborne radar," *2017 IEEE Radar Conference (RadarConf)*, Seattle, WA, USA, 2017, pp. 0903–0907.
- [6] N. Ustalli, M. N. Peixoto, T. Kraus, U. Steinbrecher, G. Krieger and M. Villano, "Experimental Demonstration of Staggered Ambiguous SAR Mode for Ship Monitoring with TerraSAR-X," *IEEE Transactions on Geoscience and Remote Sensing*, vol. 61, pp. 1–16, 2023.
- [7] M. Villano, G. Krieger, M. Jäger and A. Moreira, "Staggered SAR: Performance Analysis and Experiments with Real Data," *IEEE Transactions on Geoscience and Remote Sensing*, vol. 55, no. 11, pp. 6617–6638, Nov. 2017.
- [8] N. Ustalli and M. Villano, "Impact of Ambiguity Statistics on Information Retrieval for Conventional and Novel SAR Modes," *2020 IEEE Radar Conference (RadarConf20)*, Florence, Italy, 2020, pp. 1–6.
- [9] M. Villano and M. N. Peixoto, "Characterization of nadir echoes in multiple-elevation-beam SAR with constant and variable pulse repetition interval," *IEEE Trans. Geosci. Remote Sens.*, vol. 60, 2022, Art. no. 5215609.
- [10] N. Ustalli, G. Krieger, and M. Villano, "A low-power, ambiguous synthetic aperture radar concept for continuous ship monitoring," *IEEE J. Sel. Topics Appl. Earth Observ. Remote Sens.*, vol. 15, pp. 1244–1255, 2022.
- [11] M. Villano, G. Krieger, and A. Moreira, "A Novel Processing Strategy for Staggered SAR," *IEEE Geoscience and Remote Sensing Letters*, vol. 11, no. 11, pp. 1891–1895, Nov. 2014.
- [12] M. Villano, G. Krieger and A. Moreira, "Waveform-Encoded SAR: A Novel Concept for Nadir Echo and Range Ambiguity Suppression," *EUSAR 2018; 12th European Conference on Synthetic Aperture Radar*, Aachen, Germany, 2018, pp. 1–6.

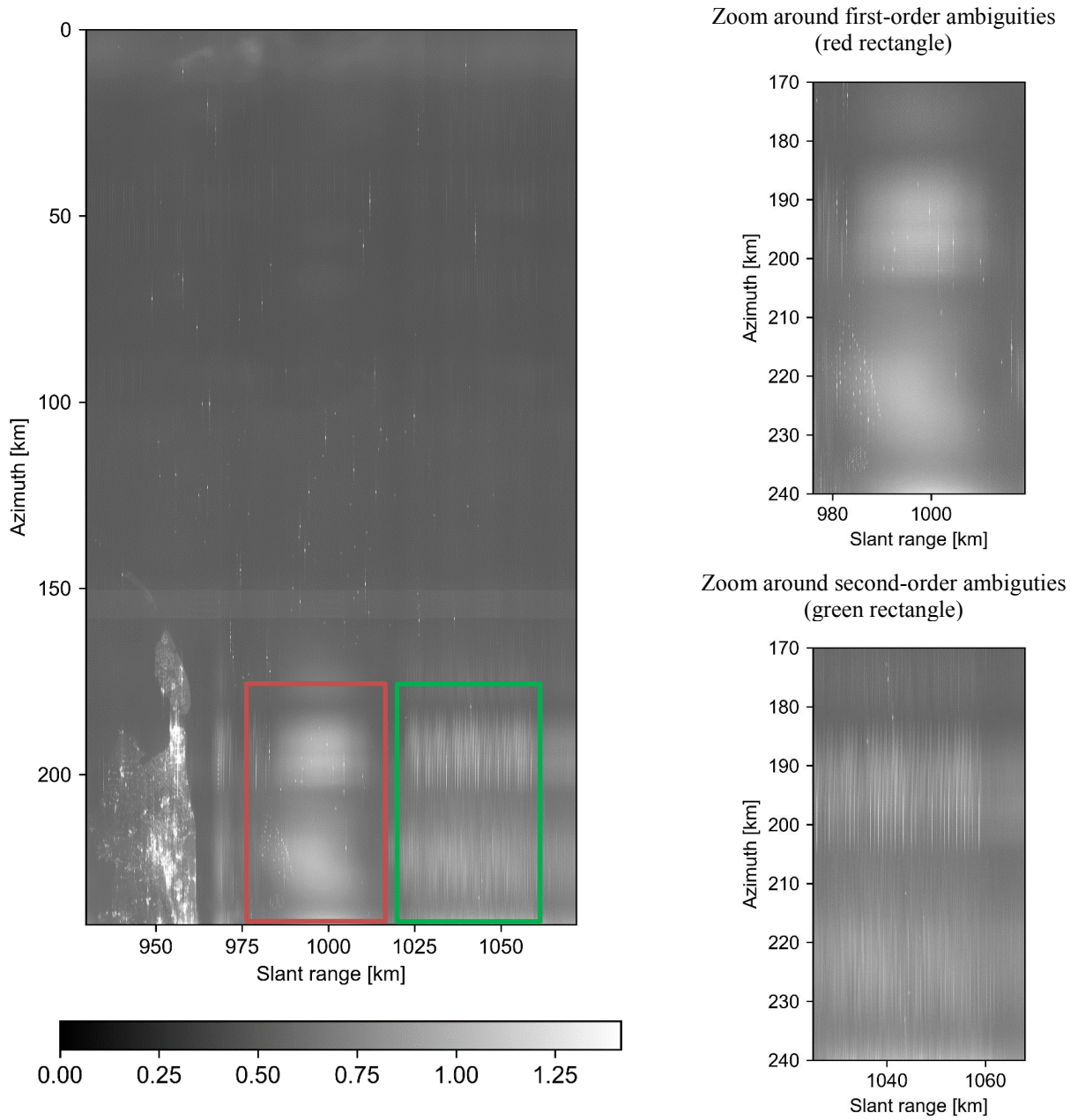


Figure 7 Intensity of the focused image acquired by TerraSAR-X in staggered ambiguous mode with alternating up- and down-chirps over the full scene. The red rectangle and the green rectangle highlight the first-order and the second-order range ambiguities from the coast.

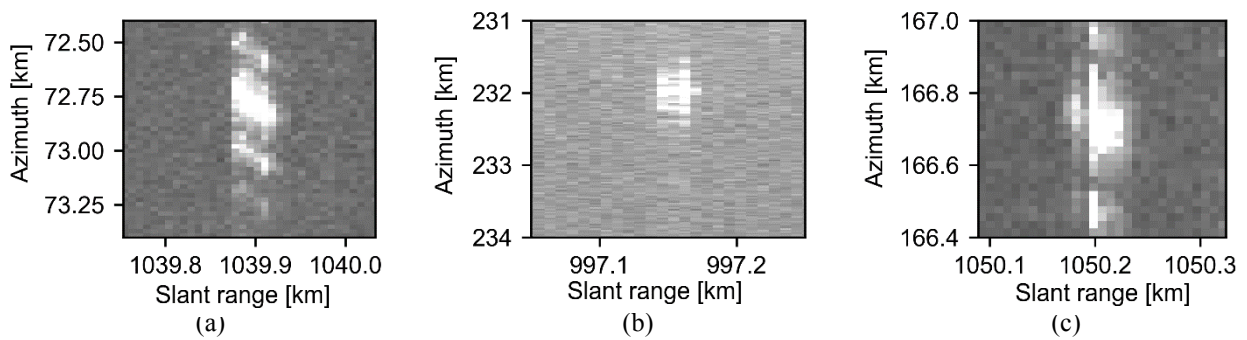


Figure 8 Zoom around medium and small ships within the scene (a) zoom around a medium ship at far range, (b) zoom around a small ship overlapped to the first-order range ambiguity of land scatterers and (c) zoom around a small ship at far range. The same colour scale as in Figure 7 is used.